

Experimental and numerical simulation as a calibration measure of a venturi tube

Abstract

The development of experimental theories has been the normal practice for studying hydraulics and fluid dynamics. Based on the fundamental equations some simplifications are included and through laboratory experimentation many of the relationships that are currently applied have been obtained. With the advancement of technology, the numerical simulation of the government equations has taken an important role in complementing the existing theories. However, it also has a certain level of simplification, so it has not been able to fully replace laboratory experimentation. A combination of both types of analysis, based on fundamental principles (theory), is necessary to obtain reliable results. In the present study, a theoretical, experimental and numerical analysis is applied to the case of flow in a Venturi tube determining that there is a high concordance when the results obtained with each of the methodologies are compared. With this, a reliable methodology is defined to analyze complex fluid flow problems.

Keywords: venturi tube, numerical simulation, experimentation, fluid dynamics, fluid flow

Volume 2 Issue 2 - 2018

Veronica Carrillo, Rubén Jerves, Franklin Lucero, Carolina Palacios, Pablo González, Andrés Chávez, Esteban Pacheco, Felipe Cisneros

Department of Civil Engineering, University of Cuenca, Ecuador

Correspondence: Veronica Carrillo, Department of Civil Engineering, University of Cuenca, Ecuador, Tel 5934051000, Email veronica.carrillo@ucuenca.edu.ec

Received: March 17, 2018 | **Published:** April 12, 2018

Abbreviation: CFD, Computational Fluid Dynamics

Introduction

Due to the complexity encountered in solving the governing equations of fluid flow, laboratory experimentation has been widely applied to develop experimental theories that help to understand and describe flow processes.^{1,2} However, experimentation has been developed mainly in idealized and simplified environments like laboratory flumes with constant discharge or one dimensional flow. Development of technology has allowed the study of increasingly more complex flow cases. Equipment that measure flow velocity in its three directions and methodologies to track fluid and sediment particles among many others are some of the advances that have allowed a better knowledge on the hydraulics of flow.³ With the application of computational fluid dynamics (CFD), the study of hydraulics and fluid dynamics has taken an important step forward. This has permitted the analysis with a very high and detailed resolution of processes such as free surface and turbulent flows, sediment transport, hydraulic structures performance, etc.^{4,5} The CFD solves numerically for a discrete domain the flow governing equations, the Navier-Stokes partial differential equations. Nonetheless, the direct solution of the governing equations is possible only in very simple cases due mainly to the high computational resources required.⁶ Therefore; simplifications have been applied to solve more complex phenomena. Even though simplifications have been verified under a variety of conditions, a level of validation and corroboration is needed to accept numerical simulations as valid.⁷ The Venturi tube is a device that uses the Venturi effect proposed by Giovanni Battista Venturi in 1797 that states the following. A tube that experiences a contraction in its cross section undergoes a pressure reduction due to the decrease of section with its corresponding increase in velocity.⁸ The applications of a Venturi Tube range from flow measurements to as a mixing device.⁹ Therefore it is important to know how it works and to determine calibration (velocity) coefficients that consent the determination of accurate flow parameters (velocity and static pressure). In the present work a

theoretical development is compared to experimental measurements and also to numerical simulation to determine the calibration coefficient of the Venturi tube of the Hydraulics and Fluid Dynamics Laboratory of the Engineering Department of University of Cuenca with the main purpose of establishing an analysis methodology that allow an integral study of any flow process in the Laboratory.

Materials and methods

Governing equations

The equations that describe the flow of fluids are known as the Navier-Stokes equations they are non-linear partial differential equations.¹⁰⁻¹² The equations for an incompressible are presented in their form of conservation of mass (continuity equation) and momentum equations (in three directions x, y, z).

Conservation of mass

$$\frac{\partial u}{\partial x} + \frac{\partial v}{\partial y} + \frac{\partial w}{\partial z} = 0 \quad (1)$$

Momentum Equations

$$\frac{\partial}{\partial t}(\rho u) + \frac{\partial}{\partial x}(\rho u^2) + \frac{\partial}{\partial y}(\rho uv) + \frac{\partial}{\partial z}(\rho uw) + \frac{\partial p}{\partial x} - \frac{\partial \tau_{xx}}{\partial x} - \frac{\partial \tau_{xy}}{\partial y} - \frac{\partial \tau_{xz}}{\partial z} = 0 \quad (2)$$

$$\frac{\partial}{\partial t}(\rho v) + \frac{\partial}{\partial x}(\rho uv) + \frac{\partial}{\partial y}(\rho v^2) + \frac{\partial}{\partial z}(\rho vw) + \frac{\partial p}{\partial y} - \frac{\partial \tau_{xy}}{\partial x} - \frac{\partial \tau_{yy}}{\partial y} - \frac{\partial \tau_{yz}}{\partial z} = 0 \quad (3)$$

$$\frac{\partial}{\partial t}(\rho w) + \frac{\partial}{\partial x}(\rho uw) + \frac{\partial}{\partial y}(\rho vw) + \frac{\partial}{\partial z}(\rho w^2) + \rho g + \frac{\partial p}{\partial z} - \frac{\partial \tau_{xz}}{\partial x} - \frac{\partial \tau_{yz}}{\partial y} - \frac{\partial \tau_{zz}}{\partial z} = 0 \quad (4)$$

Where: ρ is the fluid density, p is pressure; g is the acceleration due to gravity, $\tau_{ij} = \mu \left(\frac{\partial v_j}{\partial x_i} + \frac{\partial v_i}{\partial x_j} \right)$, and μ is the coefficient of viscosity for a Newtonian fluid.

Venturi tube operation is based on the Bernoulli's principle or Bernoulli's equation. Starting from the momentum equations with the assumptions that friction terms are considerable lower compared with the other terms in the equation, the flow is along a streamline, for permanent flow and for incompressible fluid (constant density), momentum equation results in the following form.¹

$$z + \frac{P}{\gamma} + \frac{v^2}{2g} = constant \text{ or}$$

$$z_1 + \frac{P_1}{\gamma} + \frac{v_1^2}{2g} = z_2 + \frac{P_2}{\gamma} + \frac{v_2^2}{2g} \tag{5}$$

Applying eq. (5) to the normal (section 1) and contracted (section 2) sections of a Venturi tube the following relation for the theoretical velocity in section 2 is obtained.

$$V_2 = \sqrt{\frac{2g(h + (p_1 + p_2) / \gamma)}{1 - \left(\frac{d_2}{d_1}\right)^4}} \tag{6}$$

Where: h is the differential position between normal and contracted section, p₁ and p₂ normal and contracted section pressure, γ fluid specific weight and d₁ and d₂ normal and contracted diameter. Since Bernoulli's equation does not consider friction effects the obtained velocity is theoretical. The real value of the contracted velocity has to be determined for each Venturi tube since it will depend on Venturi's dimensions, material and form. To make real the theoretical velocity, it is multiplied by a correction factor denominated as discharge coefficient C_d.

$$V_{2r} = C_d V_2 \tag{7}$$

Experimental configuration

The experimental simulations were performed in the Hydraulics and Fluid Dynamics Laboratory of the Civil Engineering Department of University of Cuenca. The equipment used is the Armfield Fluid Friction Measurements unit (Armfield C6MkII). The pipes system includes, among others devices, a Venturi tube that allows the simulation of the flow throughout it as well as the measurement of parameters such as the pressure in the normal and contracted sections. In Figure 1 the pipe system and the Venturi tube detail are shown. The experimental configuration comprises a pump and a recirculation system. Five experiments with different discharges were planned. In Table 1 the discharge values simulated are presented. The devices shown in Figure 1 allow the measurement of the pressure value in the interest points (normal and contracted sections).

Table 1 Experimental discharge values

Experiment	Discharge (l/s)
1	0.204
2	0.355
3	0.49
4	1.011
5	1.216

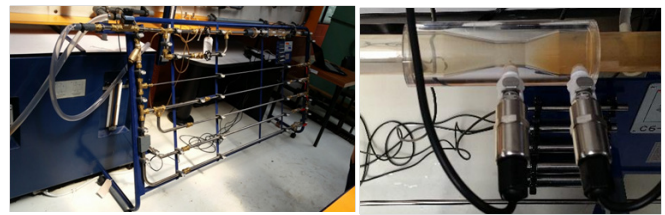


Figure 1 Venturi tube structure.

Numerical simulation

The CFD is used to simulate numerically the flow through the Venturi. The CFD software package used is OpenFOAM an open source code. The numerical method used by OpenFOAM in the present simulation is the finite volume method and the solver is icoFoam. The Gauss linear scheme is used for the gradient, divergence, and laplacian operators. The interpolation scheme is set to linear. Additionally, for the component of gradient normal to a cell face the option orthogonal is selected. The Gauss linear scheme used has second order of accuracy.¹³ Therefore, the results have a second order precision. Simulations were considered converged when the residuals for the continuity, pressure, and momentum equations drop below the value of 1×10⁻⁶.

Domain and boundary conditions

The simulated domain comprises the contraction part of the Venturi. Explicitly, it starts with the normal section with a diameter of 2.40cm and the contraction to a diameter of 1.40cm is produced in 2.6cm. The boundary conditions used for all simulations were: along the central axis of the Venturi an axisymmetric boundary condition was enforced. The device walls were given a wall no-slip or zero velocity condition. The entrance was given a constant uniform velocity corresponding to each of the fives discharges considered. Finally, to the domain outlet, a zero pressure value was assigned. Three consecutive finer meshes were considered for the numerical simulation along the symmetry axis (2.60cm in x direction) 20, 40 and 80 numbers of cells were used. In Figure 2 a detail of the domain for the coarsest mesh is presented.

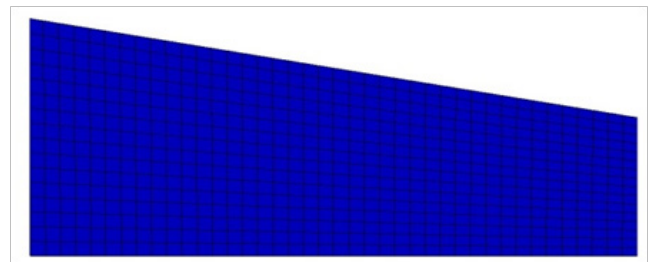


Figure 2 Numerical Simulation domain (coarsest mesh).

Grid Convergence Index

The Grid Convergence Index (GCI) is used to determine whether the grid independence has been reached.¹⁴ It permits to quantify the error due to domain discretization. A range of certainty can be determined for the solution obtained with the fine grid. This range constitutes the range that would contain the exact solution with a reliable probability.¹⁵ The GCI is determined with the following expression.

$$GCI [fine\ grid] = F_s \frac{|\epsilon|}{r^s - 1} \tag{8}$$

$$\varepsilon = \frac{f_2 - f_1}{f_1} \tag{9}$$

Where, F_s is the factor of safety of the method, r is grid refinement ratio (h_2/h_1), s is the order of accuracy of the numerical solution f_1 and f_2 corresponds to the numerical solution with different grid resolution refined with s factor. Recommendations for F_s state values from 1.0 to 3.15. Depending on the level of uncertainty present on the simulation this value has to be assumed. A value of 3.0 can be seen as a conservative value required in cases of high uncertainty. However, this value can be reduced when a better knowledge of the simulated processes is had. Moreover, in the cases when three consecutive finer meshes are used a factor of 1.25 can be used.¹⁶

Results and discussion

Experimental simulation

As stated before, five experimental simulations were performed.

Table 2 Experimental simulations results

Experiment	Discharge (l/s)	Velocity (m/s)		Pressure (meters head)	
		Normal	Contracted	Normal	Contracted
1	0.204	0.451	1.326	21.822	21.699
2	0.355	0.785	2.307	21.013	20.721
3	0.49	1.083	3.184	20.02	19.482
4	1.011	2.235	6.569	13.219	11.12
5	1.216	2.688	7.901	9.12	6.067

Table 3 Theoretical results

Theoretical	Discharge (l/s)	Velocity (m/s)		Pressure (meters head)	
		Normal	Contracted	Normal	Contracted
1	0.204	0.451	1.326	21.822	21.743
2	0.355	0.785	2.307	21.013	20.773
3	0.49	1.083	3.184	20.02	19.563
4	1.011	2.235	6.569	13.219	11.274
5	1.216	2.688	7.901	9.12	6.306

Numerical simulation

Applying OpenFoam solver icoFoam and the conditions stated before the numerical simulations were performed. All the five cases were also simulated numerically. The results are shown in Table 4. In Figure 3 pressure and velocity distribution along the domain obtained with the numerical simulation is shown. Comparing V_2 and p_2 for all three types of analysis and considering the experimental simulation as the comparison parameter the following can be punctuated. There is not exist accountable differences between theoretical and numerical results. This is due to the fact that the same assumptions are made to obtain Bernoulli's equation (no friction effects) and for the numerical

With a given discharge and for the normal and contracted cross section the normal and contracted velocities were calculated. Measurements of the pressure were taken for the normal and contracted sections. In Table 2 the experimental results are presented.

Theoretical analysis

Using eq. (6) and reorganizing its terms, an equation to determine $\Delta p(p_1 + p_2)$ is obtained as follows.

$$\Delta p = \frac{V_2}{\sqrt{1 - \left(\frac{d_2}{d_1}\right)^4}} \sqrt{\frac{2g}{2g}} \tag{10}$$

With the dimensions of the Venturi Δp was determined. Considering p_1 (taken from the experimental measurements) p_2 was calculated for the theoretical analysis (Table 3).

model (smooth boundary without friction effects). The greatest error or difference registered correspond to p_2 (or differential pressure) when experimental and theoretical values are compared. This error is 4%. For the contracted velocity the greatest error registered is 2%. In Figure 4 a graphical comparison is presented. The GCI calculation was performed with discharge 2 (0.355 l/s). As can be observed in Table 5 all three grid resolutions used have given the same differential pressure. This means that grid independence has been reached and the error due to discretization has been eliminated. The results from coarsest mesh can be used with a higher level of certainty avoiding the computational cost of simulating the intermediate or finest mesh.

Table 4 Numerical simulation results

Numerical simulation	Discharge (l/s)	Velocity (m/s)		Pressure (meters head)	
		Normal	Contracted	Normal	Contracted
1	0.204	0.451	1.325	21.822	21.742
2	0.355	0.785	2.299	21.013	20.771
3	0.49	1.075	3.157	20.02	19.553
4	1.011	2.219	6.503	13.219	11.243
5	1.216	2.649	7.743	9.12	6.282

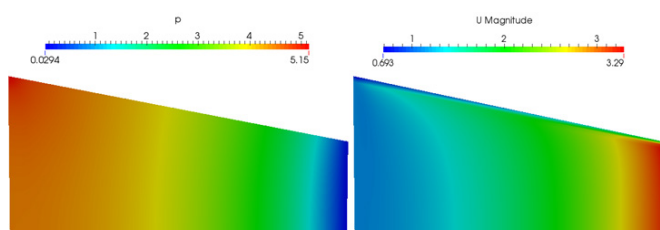


Figure 3 Pressure and velocity distribution along the domain.

Table 5 Differential pressure numerical results with different grid resolution

Number of cells	Δp (water head)
20	0.240
40	0.240
80	0.240

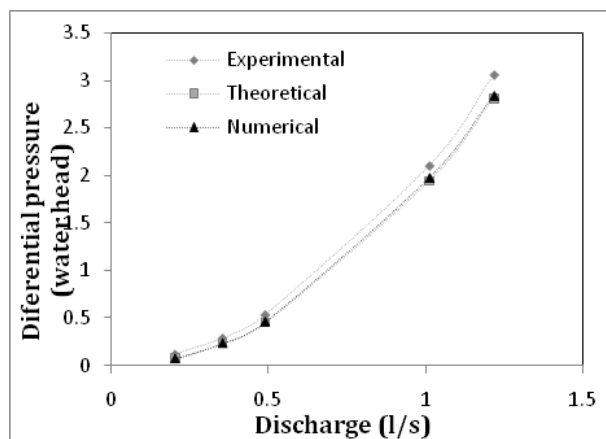


Figure 4 Experimental, Theoretical, and Numerical Simulations comparison.

Conclusion

Theoretical, experimental, and numerical analyses were performed to simulate flow characteristics of a Venturi tube. Negligible differences were reported between theoretical and numerical simulations. On the other hand, experimental simulations show greater “error” values. However, the differences registered are lower than 5%. In laboratory

procedures some level of error is expected due to Laboratory configurations. In the present study an analysis methodology has been applied using three important axes of hydraulics and fluid dynamics studies. Some theoretical developments rely on hypothesis and simplifications that not always fit real conditions. Experimental procedures some times are idealized representation of real phenomena. Numerical simulations solve the governing equations. However, a level of simplification is always present. Therefore, an integrated analysis that contains the contribution of these three main axes reduces the uncertainty and strengthens the results.

Acknowledgment

None

Conflict of interest

The authors declare no conflict of interest.

References

- Streeter VL, Wylie EB, Bedford KW. Fluid mechanics, 9th edition. Boston: WCB/McGraw Hill; 1998.
- Yost SA, Rao PMSV. A non-oscillatory scheme for open channel flows. *Adv Water Resour.* 1998;22(2):133–143.
- Guo JJ. Advances in Hydraulics and Water Engineering: proceedings of the 13th IAHR-APD congress, Singapore, 6 - 8 August 2002. International Association for Hydraulic Engineering and Research, Singapore: World Scientific; 2002.
- Wu W, Rodi W, Wenka T. 3D Numerical Modeling of Flow and Sediment Transport in Open Channels. *J Hydraul Eng.* 2000;126(1):4–15.
- Faure JB, Buil N, Gay B. 3-D Modeling of unsteady free-surface flow in open channel. *J Hydraul Res.* 2004;42(3):263–272.
- Shi J, Thomas TG, Williams JJR. Free-Surface Effects in Open Channel Flow at Moderate Froude and Reynold’s Numbers. *J Hydraul Res.* 38(6):465–474.
- Oreskes N, Shrader FK, Belitz K. Verification, Validation, and Confirmation of Numerical Models in the Earth Sciences. *Science.* 1994;263(5147):641–646.
- Street RL, Watters GZ, Vennard JK. Elementary fluid mechanic. 7th edition. New York: J Wiley; 1996.
- Oliveira JLG, Passos JC, Verschaeren R, et al. Mass flow rate measurements in gas–liquid flows by means of a venturi or orifice plate coupled to a void fraction sensor. *Exp Therm Fluid Sci.* 2009;33(2):253–260.

10. Acheson DJ. Elementary fluid dynamics. Oxford : New York: Clarendon Press ; Oxford University Press; 1990.
11. Batchelor GK. An introduction to fluid dynamics. Cambridge: Cambridge Univ Press; 2010.
12. Panton RL. Incompressible flow, Fourth edition. Hoboken, New Jersey: Wiley; 2013.
13. OpenFOAM. OpenFOAM The Open Source CFD Toolbox, User Guide. Open FOAM Foundation; 2014. p. 1–220.
14. Roache PJ. Perspective: A Method for Uniform Reporting of Grid Refinement Studies. *J Fluids Eng.* 1994;116(3):405.
15. Celik, Zhang WM. Calculation of Numerical Uncertainty Using Richardson Extrapolation: Application to Some Simple Turbulent Flow Calculations. *J Fluids Eng.* 1995;117(3):439.
16. Roache PJ. Verification and validation in computational science and engineering. Albuquerque, NM: Hermosapublishers; 1998.